Available online at www.sciencedirect.com

ScienceDirect

Procedia Engineering 102 (2015) 1016 – 1025

Procedia Engineering

www.elsevier.com/locate/procedia

The 7th World Congress on Particle Technology (WCPT7)

Particle Distribution Studies in Highly Concentrated Solid-Liquid Flows in Pipe using the Mixture Model

R. Silva[a], C. Cotas[a], F. A. P. Garcia[a], P. M. Faia[b], M. G. Rasteiro[a]*

[a]*CIEPQPF, Department of Chemical Engineering, University of Coimbra, Rua Sílvio Lima, Polo II, 3030-790 Coimbra – Portugal*
[b]*Department of Electric and Computers Engineering, University of Coimbra, Rua Sílvio Lima, Polo II, 3030-790 Coimbra – Portugal*

Abstract

The hydraulic conveying of solid-liquid concentrated suspensions in pipelines corresponds to complex flows where particles with different sizes, concentrations and flow velocities exhibit different flow regimens. Predicting their behavior is fundamental for the adequate design of pumping equipment and flow rigs. In traditional numerical approaches the turbulence production is assumed to be directly dependent on the increase of the particle size; this contradicts data from the literature where small particles cause an augmentation of turbulence and medium size particles attenuate turbulence. Also, in the traditional approach the same drag correlation is assumed to account for particle-fluid interaction in different flow regimes, which, in the case of turbulence augmentation and attenuation can differ considerably. In the present work numerical studies were conducted to simulate highly concentrated flows of settling medium sized particles using a Mixture Model, incorporating a Low Reynolds turbulence closure and a Schiller-Naumann drag correlation to depict the flow of concentrated solid-liquid suspensions. Since not all particle distributions were accurately portrayed, different drag correlations were implemented to provide a more adequate representation of the relative velocity between phases and particle distributions. Amongst the drag correlations implemented the Schiller & Naumann showed the best agreement for the highest particle concentrations at intermediate velocities, whilst the Haider & Levenspiel displayed the best fit with the experimental data for the highest flow velocities and particle concentrations. The Gidaspow-Schiller-Naumann drag correlation was more adequate for low flow velocities and with intermediate particle concentrations. With this work it is shown that using the same drag correlation for the numerical description of experimental data for highly concentrated settling solid-liquid flows does not adequately reproduce the different flow regimes.

Selection and peer-review under responsibility of Chinese Society of Particuology, Institute of Process Engineering, Chinese Academy of Sciences (CAS)

Keywords: drag model; slip velocity; mixture model; turbulence modification; settling solid-liquid flows;

* Corresponding author. Tel.: +351 239 798 700; fax: +351 239 798 703.
E-mail address: mgr@eq.uc.pt

Selection and peer-review under responsibility of Chinese Society of Particuology, Institute of Process Engineering, Chinese Academy of Sciences (CAS)
doi:10.1016/j.proeng.2015.01.224

1. Introduction

The conveying of particles in pipelines is of pivotal importance in industrial applications such as the production of chemicals, pharmaceuticals or foodstuffs, as also in the transportation of minerals and wastes. In these applications an array of different particle sizes and concentrations can be found, displaying unique behaviors and originating very different flow regimes. The hydraulic conveying of solid-liquid concentrated suspensions is a typical example where particles with different sizes, concentrations and flow velocities exhibit complex flow regimens. Predicting their behavior is fundamental for the adequate design of pumping equipment and flow rigs.

In traditional numerical approaches the turbulence production is assumed to be directly dependent on the increase of the particle size; however this contradicts data from the literature where small particles cause an augmentation of turbulence and medium size particles attenuate turbulence [1,2]. Also, in the traditional approach the same drag model is assumed to account for particle-fluid interaction in different flow regimes and particle distributions, which, in the case of turbulence augmentation and attenuation can be quite different. Indeed, drag models are derived to depict a single particle behavior [3] in fluids which in systems where multiple particles are present, where particle-particle interactions are predominant, become inadequate. In this regard, several authors have presented modifications to existing drag models to account for high solid fractions and particle interactions [3-6].

In the present work numerical studies on highly concentrated flows of settling medium sized particles were conducted, where a wide range of flow regimens is observed depending on the flow velocity and particle concentration; for low velocities a stationary bed is formed, for intermediate flow velocities either a moving bed or heterogeneous regime are observed and for higher flow velocities a quasi-homogeneous regime is usually expected [7]. A Mixture Model, with a Low Reynolds turbulence closure [8] and incorporating initially a Schiller-Naumann slip model [9], was employed to depict the behavior of a concentrated solid-liquid flow of medium sized particles for the different flow regimens. This approach, although providing reliable representations of the vertical distributions of particles in the pipeline for some of the flow regimes, presented significant deviations for others. Since not all particle distributions were accurately portrayed, different drag models were implemented to provide a more adequate representation of the relative velocity between phases and of the particle distributions for those flow regimes. Amongst the drag models implemented the Schiller & Naumann model showed the best agreement for the highest particle concentrations at high flow velocities, while the Haider & Levenspiel model displayed the best fit with the experimental data for the medium flow velocities and highest particle concentrations. Meanwhile, the Gidaspow-Schiller-Naumann model was more adequate for low flow velocities and with intermediate particle concentrations. With this work it is shown that the use of the same drag model for the representation of experimental data for highly concentrated settling solid-liquid flows is not adequate to reproduce particles behavior at different flow regimes.

Nomenclature

ε	kinetic energy dissipation rate for high Reynolds closure
$\tilde{\varepsilon}$	kinetic energy dissipation rate for Low Reynolds closure
μ	mixture dynamic viscosity
μ_c	dynamic viscosity of the continuous phase
μ_d	dynamic viscosity of the dispersed phase
μ_T	turbulent dynamic viscosity
ν	mixture kinematic viscosity
ρ	mixture density
ρ_c	continuous phase density
ρ_d	dispersed phase density
σ_T	particle Schmidt Number
τ_{Gm}	turbulent and viscous stresses
ϕ_c	continuous phase volumetric fraction
ϕ_d	dispersed phase volumetric fraction
c_d	dispersed phase mass fraction
C_D	drag coefficient

Cv	local solids concentration
Cvf	efflux concentration
D	low Reynolds damping function
D_{md}	turbulent eddy diffusion
D_{pipe}	pipe internal diameter
d_p	particle diameter
D_t	turbulent mass diffusion
E	low Reynolds damping function
F	volume forces
g	gravitational acceleration
I	identity matrix
k	turbulent kinetic energy
L	pipe length
m_{dc}	mass transfer ratio between phases
p	Pressure
Re_p	particle Reynolds Number
u	mixture velocity
u^T	transpose of the mixture velocity
u_{SLIP}	relative velocity between phases
u_c	continuous phase velocity
u_d	dispersed phase velocity

2. Previous Work

A survey in the literature will reveal several studies on the influence of drag correlations in the accurate numerical representation of particle distribution in vessels. Visuri et al (2012) [6] employed several models commonly used in the literature to study solid-liquid fluidized systems. Some of those models were specifically developed for other systems: however they felt that their extension outside of their specificity was of greater value for the study. From the drag models considered, either purely theoretical, experimental or a combination of both, the authors concluded that in CFD there is no universal drag model since they are case specific. Lareo et al (1997) [3] have conducted a very thorough review on drag models for both single and multiparticle systems in Newtonian and Non-Newtonian fluids for solid-liquid food flows. Hadinoto (2010) [4] and Hadinoto & Chew (2010) [5] conducted studies on turbulence modulation for dilute solid-liquid systems that showed that using different combinations of drag correlations and turbulent closures is needed to correctly identify the dependence of fluid-particle interactions with the Reynolds number. Pang and Wei (2011) [10] analyzed key factor in both drag and lift correlations for bubbly flow systems highlighting the difficulty in choosing adequate drag and lift correlations, also stressing the pivotal importance in properly modelling interphase forces in complex two-phase flows. A similar study for blood flow was undertook by Yilmaz and Gundogdu [9] where the authors state the importance of powerful drag-lift models for flows with complex phenomena like deformation, geometry, concentration and aggregation.

3. Mixture Model Theory

The Mixture Model is a two fluid Euler-Euler model [8,11], in which the phases consist of a dispersed phase (solid particles, liquid droplets, etc) and a continuous phase (liquid). It is translated by a continuity equation for each phase and a momentum equation for the mixture, where an additional term is included to describe the effect of the velocity differences between the phases. The Mixture Model is more advantageous, when compared with a Lagrangian model, due to the considerable smaller amount of variables to be determined. Common used simplifications are that in the dispersed phase all particles consist of spherical particles of a single average size and that particle-interactions are frequently negligible [8,11]. Its application is conditioned by the following assumptions: each phase density is constant, both phases share the same pressure field, and the velocity difference between phases

is determined assuming that pressure, gravity and viscous drag are all balanced. The momentum equation for the mixture is given by

$$\rho u^T + \rho(u \cdot \nabla)u = -\nabla p - \nabla \cdot \left(\left(\rho c_d (1 - c_d) \right) u_{SLIP} u_{SLIP} \right) + \nabla \cdot \tau_{Gm} + \rho g + F \tag{1}$$

The mixture velocity and density are defined in Equations (2) and (3), respectively

$$u = \frac{\phi_c \rho_c u_c + \phi_d \rho_d u_d}{\rho} \tag{2}$$

$$\rho = \phi_c \rho_c + \phi_d \rho_d \tag{3}$$

and consequently the dispersed phase mass fraction is given by

$$c_d = \frac{\phi_d \rho_d}{\rho} \tag{4}$$

The velocity between phases is expressed as

$$u_d - u_c = u_{cd} = u_{SLIP} - \frac{D_{md}}{(1 - c_d)} \nabla \phi_d \tag{5}$$

Different drag correlations for the slip velocity calculation will be addressed in the next section. If no turbulence is present, then there is no turbulence dispersion and the last term in the right side of Equation (5) is zero,

$$D_{md} = \frac{\mu_T}{\rho \, \sigma_T} \tag{6}$$

with

$$\sigma_T = \frac{\nu}{D_t} \tag{7}$$

The Schmidt Number for a particle in turbulent flow, σ_T, is usually accepted to be in the interval between 0.35 and 0.7. In most commercial codes the value is 0.35. According to Reynolds [12] the Schmidt Number for a particle in turbulent conditions, is defined as being the ratio between the kinematic viscosity, ν, and the turbulent mass diffusion, D_t , as in Equation (7). The total stress, τ_{Gm}, which incorporates the turbulent and viscous stresses, is given by

$$\tau_{Gm} = (\mu + \mu_T)[\nabla \mathrm{u} + \nabla u^T] - \frac{2}{3} \rho k I \tag{8}$$

where μ_T is the turbulent viscosity (see Equation (16)). The transport equation for the dispersed phase mass fraction, ϕ_d, is presented in Equation (9)

$$\frac{\partial}{\partial t} (\phi_d \rho_d) + \nabla \cdot (\phi_d \rho_d u_d) = -m_{dc} \tag{9}$$

The continuous phase mass fraction ϕ_c equals

$$\phi_c = 1 - \phi_d \tag{10}$$

The mixture continuity equation becomes

$$\rho_t + \nabla \cdot (\rho u) = 0 \tag{11}$$

Since one of the assumptions of the Mixture Model is that the densities of each phase, ρ_c and ρ_d, are constant, then combining Equations (9) and (10), allows Equation (11) to be rewritten

$$\rho_c - \rho_d \left[\nabla \cdot (\phi_d(1-c_d)u_{SLIP} - D_{md}\nabla\phi_d) + \frac{m_{dc}}{\rho_d}\right] + \rho_c(\nabla \cdot u) = 0 \tag{12}$$

The velocity between phases, $\boldsymbol{u_{slip}}$, can be obtained using empirical drag correlations. In the next sub-sections the drag correlations employed in this study are presented.

3.1. Schiller-Naumann (SN) Correlation

The *Schiller-Naumann* correlation [10] correlation is one of the most employed drag correlations in the last decades [6] and uses the following relationship for the calculation of the drag coefficient, C_D.

$$C_D = \begin{cases} \frac{24}{Re_p}\left(1 + 0.15Re_p^{0.687}\right) & if\ Re_p > 1000 \\ 0.44 & if\ Re_p < 1000 \end{cases} \tag{13}$$

3.2. Haider & Levenspiel (HL) Correlation

In the literature [1] the *Haider & Levenspiel* correlation has been employed to a wide range of data from different sources and this correlation showed better results than the remaining.

$$C_D = \frac{24}{Re_p}\left(1 + 0.1806\, Re_p^{0.6459}\right) + \frac{0.4251}{1 + \left(\frac{6880.95}{Re_p}\right)} \qquad if\ \ Re_p < 2.6 \times 10^5 \tag{14}$$

3.3. Gidaspow-Schiller-Naumann (GSN) Correlation

The Gidaspow-Schiller-Naumann (GSN) correlation [6,10] is an extension to the aforementioned (SN) correlation, however, contrarily to the (SN) correlation it was developed to account for the presence of several particles.

$$C_D = \begin{cases} \frac{24}{(1-\phi_s)Re_p}\left(1 + 0.15((1-\phi_s)Re_p)^{0.687}\right) & (1-\phi_s)Re_p > 1000 \\ 0.44 & (1-\phi_s)Re_p < 1000 \end{cases} \tag{15}$$

3.4. Launder-Sharma Low Reynolds k-ε Turbulence Model

The Low Reynolds k-ε Turbulence Model incorporated in the Mixture Model was the Launder-Sharma model (LS). It was the first published as Low Reynolds model and this was the basis for its choice. The Low Reynolds k-ε Turbulence Models is an attempt to model directly the influence of viscosity in the flow, through the integration of the turbulence equations all the way to the wall [14-16]. Turbulent flows are modeled, again, using transport equations for the Turbulent Kinetic Energy k (Equation (17)), the Dissipation Rate ε (Equation (18)) (with $\tilde{\varepsilon} = \varepsilon - D$ as the pseudo dissipation rate, for computational convenience, allowing setting it equal to zero at the pipe wall), and together with the Prandtl-Kolmogorov turbulent viscosity expression (Equation (16)), all this composing the general formulation of the Launder-Sharma Low Reynolds k-ε Turbulence Model, which is incorporated in the Mixture Model. The Low Reynolds model strays from the Standard/High Reynolds model through the inclusion of viscous diffusion in all the transport equations. The damping functions (Table 1) and boundary conditions introduce the local level of turbulence, and, lastly the terms D and E are employed to represent the near-wall behavior of turbulence [14-16].

$$\mu_T = \rho\, C_\mu f_\mu \frac{k^2}{\varepsilon} \tag{16}$$

$$\rho \frac{\partial k}{\partial t} + \rho u \cdot \nabla k = \nabla \cdot \left(\left(\mu + \frac{\mu_T}{\sigma_k}\right)\nabla k\right) + \mu_T\left(\nabla u : (\nabla u + (\nabla u)^T) - \frac{2}{3}(\nabla \cdot u)^2\right) - \frac{2}{3}\rho\, k\, \nabla \cdot u - \rho\, \varepsilon - \rho\, D \tag{17}$$

$$\rho \frac{\partial \varepsilon}{\partial t} + \rho u \cdot \nabla \varepsilon = \nabla \cdot \left(\left(\mu + \frac{\mu_T}{\sigma_\varepsilon} \right) \nabla \varepsilon \right) + f_1 C_{\varepsilon 1} \frac{\varepsilon}{k} \mu_T \left(\nabla u : (\nabla u + (\nabla u)^T) - \frac{2}{3} (\nabla \cdot u)^2 \right) - \frac{2}{3} \rho k \nabla \cdot u - f_2 C_{\varepsilon 2} \frac{\varepsilon^2}{k} + \rho E \quad (18)$$

The closure coefficients employed were: $C_{\varepsilon 1}$=1.44; $C_{\varepsilon 2}$=1.92; C_μ=0.09; σ_k=1.0; σ_ε=1.3; and the Low Reynolds damping functions, as well as boundary conditions, are presented in Table 1.

Table 1. Low Reynolds k-ε damping functions and boundary conditions.

f_μ	f_1	f_2	D	E	Re_T	k_{wall}	$\tilde{\varepsilon}_{wall}$
$e^{\left(-\frac{2.5}{1+\frac{Re_t}{50}}\right)}$	1	$1 - 0.3\, e^{(-Re_t{}^2)}$	$2\upsilon \left(\frac{\partial^2 \sqrt{k}}{\partial x_j}\right)^2$	$2\upsilon\upsilon_t \left(\frac{\partial^2 u_i}{\partial x_j \partial x_k}\right)^2$	$\frac{k^2}{\nu\, \varepsilon}$	0	0

4. Experimental Conditions

Experimental data from the literature [1] served as the reference for the CFD simulations presented in this work. Inertial medium sized particles with a diameter of 0.44 mm and increasing solid volumetric fractions were implemented until a maximum value of 0.4, which is a highly concentrated flow. In all the experiments a particle bed was observed, with its height increasing with solid concentration and decreasing with increasing flow velocities. For the data with these particles the pressure drop per meter was very similar for all solid concentrations, at the highest flow velocities, indicating a turbulence attenuation resulting from the presence of the particles [17,18], which resulted in pressure drop values very close to the pressure drop for water flows under the same conditions.

Table 2. Experimental conditions for the particle flow.

D_{pipe} [m]	5.49 x10^{-02}
L [m]	1
ρ_s [kg/m^3]	2470
ρ_f [kg/m^3]	998
μ_f [Pa.s]	1.02 x10^{-03}
dp [mm]	0.44
ϕ_d	0.3 ; 0.4
V_{in} [m/s]	2; 3 ; 5

4.1. FEM Mesh

The finite element meshes (FEM) employed in the numerical studies were refined until mesh independent results were obtained. For the numerical studies with the Mixture Model and a Launder-Sharma Low Reynolds k-ε turbulence model (MM+LR) a value of 1 for the dimensionless wall distance was employed (Table 3).

Table 3. Mesh parameters.

	MM+LR
Number of elements	3 224 961
Number of Boundary Layers	6
Dimensionless wall distance (y^+)	1

5. Results & Discussion

5.1. Solids Volumetric Fraction of 0.4

In the following images the numerical results for the vertical particle distribution, drag coefficient and slip velocity (velocity between phases) are presented for the highest particle volumetric concentration of 0.4 and for 3

and 5 m/s flow velocities. In Figure 1, the numerical profiles for the vertical solids distribution profiles obtained with the drag correlations are compared with experimental data [1].

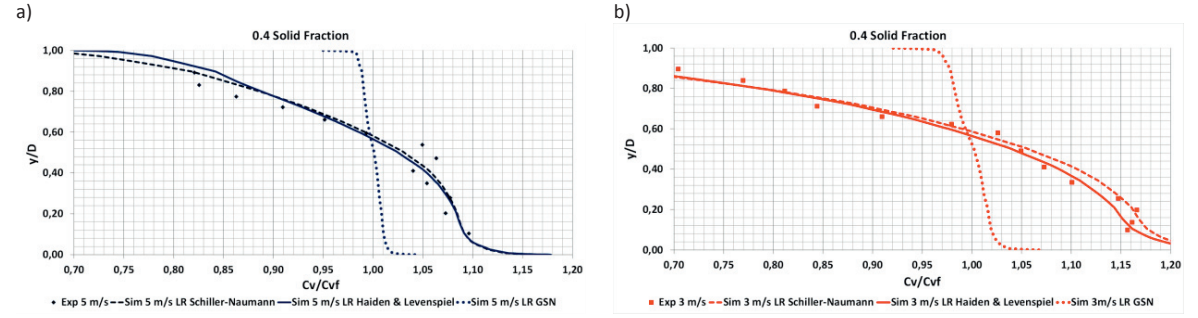

Fig.1. Adimensional numerical vs experimental vertical particle distribution profiles (a) for a flow velocity of 5 m/s; (b) for a flow velocity of 3 m/s with a particle volumetric fraction of 0.4.

Comparing the profiles for the two flow velocities in Figure 1 we can see some differences, between the two flow velocities: near the bottom the drag correlation's numerical results are identical and diverge near the top of the pipe for the high flow velocity (5 m/s) and vice-versa for the medium flow velocity (3 m/s). It is obvious that the (GSN) drag correlation is inadequate for both flow velocities at this particle concentration; as for the high flow velocity the (SN) drag correlation seems to depict more accurately the experimental particle distribution profiles and the (HL) drag correlation performs better for medium flow velocities (3 m/s). The (GSN) drag correlation inability to represent the experimental profiles could be related to the fact that it only performs accurately for solid volumetric fractions below 20% [6]. In spite being developed to account for particle-particle interaction, through the introduction of the voidage function [6], there is an overshoot in the estimation of the fluidization of the particles.

For the medium flow velocity (3 m/s) the (SN) drag correlation, established for a single sphere, the calculated results loose quality towards the bottom of the pipe, where the moving bed is present and is dominated by particle-particle and particle-wall interactions with a behavior that is considerably different from a single sphere. Observing Figure 1 for both velocities the (SN) correlation seems to better describe flows where most particles are fluidized and where the particle-particle interactions are significant lower when compared with a moving bed. Similar observations have been found in the literature where the (SN) drag correlation behaves accurately for two-phase complex flows [9].

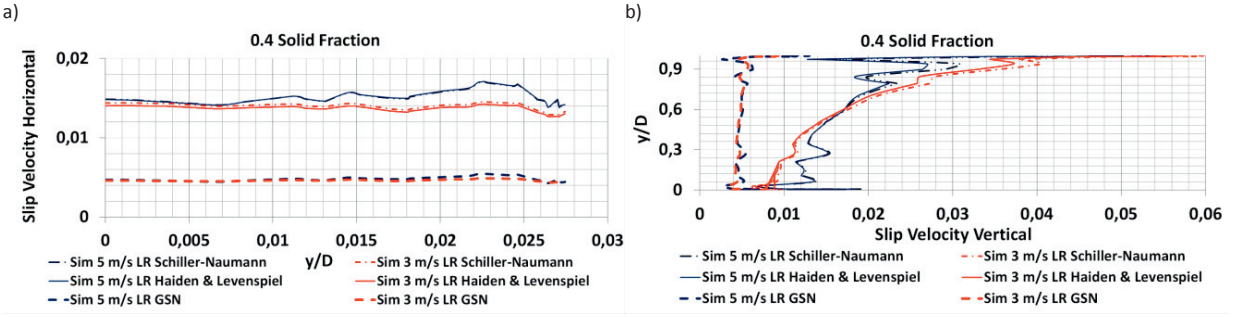

Fig.2. Numerical horizontal (a) and vertical (b) slip velocity profiles for flow velocities of 3 and 5 m/s with a particle volumetric fraction of 0.4.

The (HL) drag correlation behavior, on the contrary, performs well for regions with high particle-particle interaction as the moving bed in the pipe bottom for the low flow velocities.

Although there is no experimental data, it still is noteworthy to analyse the numerical slip velocity profiles (Figure 2) obtained with the different correlations. Again, as noted for the solids volumetric concentration profiles, the (GSN) correlation numerical data for the slip velocity for both horizontal and vertical axis, Figure 2, displays a behaviour that differs significantly from the other drag correlations. This, in conjunction with the experimental and

numerical results for particles concentration in Figure 1, seems to further demonstrate that the (GSN) drag correlation is inadequate for these flows. This is even more noticeable in the medium flow velocity (3 m/s) for which the numerical slip profiles obtained with the (GSN) correlation display an almost homogeneous behaviour with a near zero slip velocity and practically uniform in the vertical direction. Both (SN) and (HL) drag correlations provide similar results in both the horizontal and vertical axis, with the exception of the top of the pipe for both flow velocities. The previous analysis for the vertical solids concentration profiles agrees with the slip velocity numerical data in the vertical direction, i.e., the slip velocity is lower near the bottom for a low flow velocity (3 m/s) where the particles movement is hindered by the other particles and higher at the top of the pipe where there are fewer particles and more space. This is a good indicator of the quality of the numerical slip profiles.

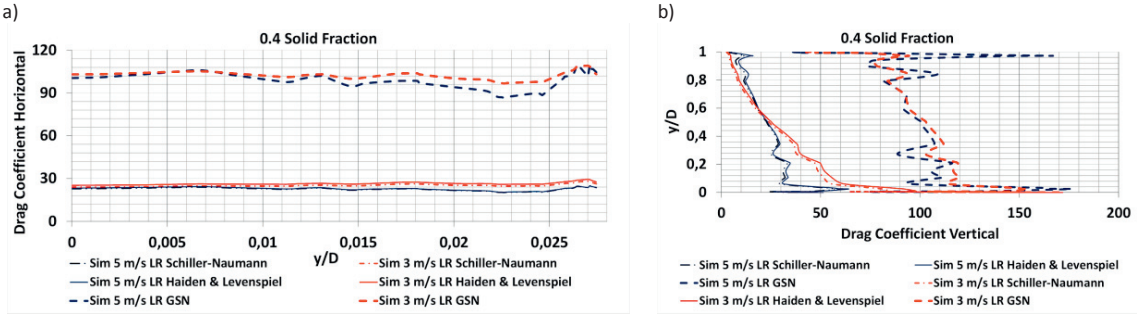

Fig.3. Numerical horizontal (a) and vertical (b) drag profiles for flow velocities of 3 and 5 m/s with a particle volumetric fraction of 0.4.

The tendencies from both the solid volumetric and slip velocity numerical profiles are reflected in the numerical drag profiles (Figure 3) for the (GSN) drag correlation. There is a considerable deviation from the remaining drag correlations in line with lack of accuracy of this correlation in depicting the experimental solid volumetric profiles. The (HL) and (SN) drag correlations provide similar values, again, for both flow velocities, when it is observable that the drag values are higher near the top of the pipe for the higher flow velocities (5 m/s), as expected, since the amount of fluidized particles is higher in this flow regime. For the medium flow velocities (3 m/s) the drag is considerable higher in the bottom of the pipe since there is a moving bed regime, where particle concentration is higher, and movement is hindered by other particles. The (HL) drag numerical values are slightly higher at the pipe bottom than the (SN) drag correlation but the difference is not significant. An interesting observation, and contrarily to the what happens at lowest flow velocity (3 m/s), is that the peak of the drag value for the highest flow velocity (5 m/s) occurs slightly above the pipe bottom which can be indicative that at this flow velocity the particles migrate from the wall towards the centre of the pipe, i.e. they migrate from a region with high shear rate (pipe wall) towards a region with lower shear rate when turbulence modulation occurs. This phenomenon has been described in the literature [17,18].

5.2. Solids Volumetric Fraction of 0.3

Since there is no data [1] below 3 m/s flow velocity for the previous solids volumetric fraction, a lower solid concentration was used at a low velocity of 2 m/s, and so a different flow regime could be studied. At this velocity a stationary bed with moving particles at the bed interface was observed by the authors [1]. Although all drag correlations present deviations, particularly at the pipe center, the (GSN) drag correlation contrarily to what was observed for the previous solid concentration, now seems to provide the more adequate numerical representation of the concentration profile, specifically for the lower half of the pipe (Figure 4).

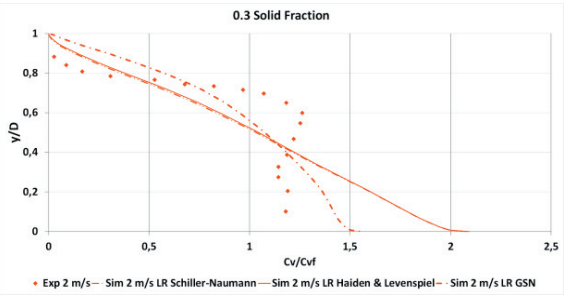

Fig.4. Adimensional numerical vs experimental vertical particle distribution profiles for a flow velocity of 2 m/s with a particle volumetric fraction of 0.3.

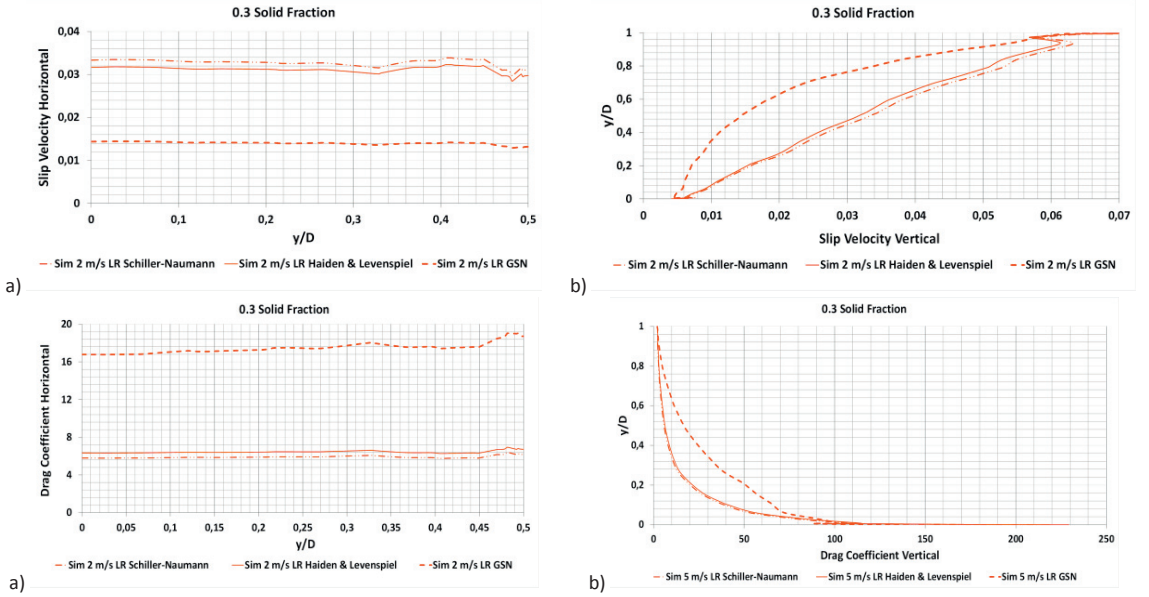

Fig.5. Numerical horizontal (a) and vertical (b) slip velocity (Top Row) and drag (Bottom Row) profiles for flow velocities of 2 m/s with a particle volumetric fraction of 0.3.

Following the same analysis as in the previous section the (GSN) correlation now provides lower values for both the horizontal and vertical numerical slip velocity values (Figure 5). Moreover, looking at the vertical drag profiles the (GSN) drag correlation presents the more sensible profile for this particle concentration with the drag being higher in the lower region, considering a stationary bed with moving particles at the bed interface regime from Figure 4 where the bulk of particles deposit occupies the lower region of the pipe. The results for the drag and slip velocity obtained with the (GSN) correlation justify the better fit obtained for the concentration profiles when using this correlation. Another important aspect is the fact that the difference between numerical slip velocity values between drag correlations is lesser than in the previous flow velocities and particle concentration.

5.3. Pressure Drop Profiles

Finally, for the pressure drop, which can be seen as a control variable in this study, at a flow velocity of 5 m/s where turbulence modulation occurs, it can be observed in Table 4 that the pressure drop values are quite similar for all drag correlations. For both velocities the (GSN) is the drag correlation that presents the biggest deviations and overall the (HL) drag correlation is the more accurate in depicting the pressure drops. For the lowest flow velocities there are still some considerable deviations which can be attributed to particle-wall friction that the Mixture Model is probably undershooting.

Table 4. Numerical vs Experimental pressure drop for 2, 3 and 5 m/s for a solid volumetric fractions of 0.3 and 0.4.

ΔP (Pa/m)	ϕ	V (m/s)	Schiller-Naumann	Haider & Levenspiel	GSN
3411.0	0.3	2	2620.9 (-23.2%)	2583.8 (-24.3%)	2336.2 (-31.5%)
3587.2	0.4	3	2838.5 (-20.8%)	2804.9 (-21.8%)	2663.9 (-25.7%)
3971.5	0.4	5	3955.9 (0.39%)	3970.6 (0.20%)	3985.9 (0.36%)

6. Conclusions

The Mixture Model, incorporating a Low Reynolds Closure, shows the capability of depicting particle behaviour when turbulence modulation occurs, for the highest flow velocities in concentrated solid-liquid flows. For the drag correlations studied so far the (HL) seems to provide the better fit for experimental pressure drop and highest solid volumetric fraction at intermediate flow velocities. The (SN) correlation also provides valid results, although, slightly less accurate than the (HL) drag correlation for the pressure drop but shows a better fit to the solids volumetric fraction profiles at highest concentrations and flow velocities. The (GSN) correlation is the least accurate drag correlation for the highest flow velocities and particle concentration which can be attributed to the fact that it was initially developed for packed beds; however, it shows the better fit for low flow velocities and intermediate particle concentrations, when a packed bed is expect to occur.

Acknowledgements

This work has been financially supported by the Fundação para a Ciência e Tecnologia, project PTDC/EQU-EQU/66670/2006, individual PhD scholarship SFRH/BD/79247/2011 and Strategic Research Center Project Pest-C/EQB/UI0102/2013.

References

[1] S.L. Lahiri, K.C. Ghanta, Slurry Flow Modelling by CFD, Chem. Ind. Chem. Eng. Q. 16(4) (2010) 295−308.
[2] C.A. Shook, Experiments with Concentrated Slurries of Particles with Densities near that of the Carrier Fluid, Can. J. Chem. Eng. 63(6) (1985) 861–869.
[3] C. Lareo, P.J. Fryer, M. Barigou, The Fluid Mechanics of Two-Phase Solid-Liquid Food Flows: A Review, Food Bio. Process. 75(2) (1997) 73-105
[4] K. Hadinoto, Predicting turbulence modulations at different Reynolds numbers in dilute-phase turbulent liquid–particle flow simulations, Chem. Eng. Sci. 65(19) (2010) 5297-5308
[5] K. Hadinoto, J.W. Chew, Modeling Fluid-Particle Interaction in Dilute-Phase Turbulent Liquid-Particle Flow Simulation, Particuology 8 (2010) 150-160.
[6] O. Visuri, G.A. Wierink, V. Alopaeus, Investigation of drag models in CFD modeling and comparison to experiments of liquid–solid fluidized systems, Int. J. Miner. Process. 104-105 (2012) 58-70.
[7] S. Peker, S. Helvaci, Solid-Liquid Two Phase Flow, first ed., Elsevier Science, 2007.
[8] COMSOL CFD Module User's Guide, Version 4.3.
[9] F. Yilmaz, M.Y. Gundogdu, Analysis of conventional drag and lift models for multiphase CFD modeling of blood flow, Korea-Aust. Rheol. J. 21(3) (2009) 161-17.
[10] M.J. Pang, J.J.Wei, Analysis of drag and lift coefficient expressions of bubbly flow system for low to medium Reynolds number, Nucl. Eng. Des. 241(6) (2011) 2204-2213.
[11] M. Manninen, V. Taivassalo, On the mixture model for multiphase flow, VTT Publications, 288, ESPOO 1996.
[12] E. Toorman, Validation of macroscopic modelling of particle-laden turbulent flows, in Proceedings 6th Belgian National Congress on Theoretical and Applied Mechanics, Gent, 26-27 May 2003.
[13] P. Brown, D. Lawler, Sphere Drag and Settling Velocity Revisited, J. Environ. Eng. 129(3):222–231.
[14] J. J. Costa, L. A. Oliveira, D. Blay, Test of several versions for the k-ε type turbulence modelling of internal mixed convection flows, Int. J. Heat Mass Tran. 42 (1999) 4391-4409.
[15] J.C.S. Lai, C.Y. Yang, Numerical simulation of turbulence suppression: Comparisons of the performance of four k-ε turbulence models, Int. J. Heat Fluid Fl. 18 (1997) 575.
[16] C.M. Hrenya, E.J. Bolio, D. Chakrabarti, J.L. Sinclair, Comparison of Low Reynolds Number k-ε Turbulence Models in Predicting Fully Developed Pipe Flow, Chem. Eng. Sci. 50 (1995) 1923.
[17] D.R. Kaushal, Y. Tomita, Experimental investigation for near-wall lift of coarser particles in slurry pipeline using γ-ray densitometer, Powder Technol. 172 (2007) 177.
[18] V. Matousek, Pressure drops and flow patterns in sand-mixture pipes, Exp. Therm. Fluid Sci. 26 (2002) 639.